Inorg. Chem. **2003**, *42*, 4165–4170

Inorganic Chemistry

Article

Synthesis and Structure of Ta_4SI_{11}: Disorder and Mixed Valency in the First Tantalum Sulfide Iodide

Mark D. Smith[†] **and Gordon J. Miller***

Department of Chemistry, Iowa State University, Ames, Iowa 50011

Received January 23, 2003

The new compound Ta_4SI_{11} has been prepared by direct reaction of the elements at 430 °C for 2 weeks in evacuated Pyrex ampules and characterized by single-crystal X-ray diffraction, X-ray photoelectron spectroscopy, magnetic susceptibility measurements, and semiempirical electronic structure calculations. Ta_4SI_{11} crystallizes with orthorhombic symmetry in space group *Pmmn*; $a = 16.135(3)$ Å, $b = 3.813(1)$ Å, $c = 8.131(2)$ Å, and $Z = 1$. The disordered structure involves two crystallographically distinct sites for Ta atoms, both of which are 50% occupied as well as a bridging anion site that is 50% S and 50% I. Magnetic susceptibility above 100 K gives $\mu_{eff} = 1.53$ μ_B to suggest one unpaired electron per formula unit. X-ray photoelectron spectroscopy and extended Hückel calculations suggest that the structure consists of Ta_3 triangles and "isolated" Ta atoms, leading to the formulation $(Ta_3)^{9+}(Ta^{4+})(S^{2-})(I^-)_{11}$ and we hypothesize that each Ta_3 is capped by a sulfur atom.

Introduction

The number of well-characterized ternary tantalum chalcogenide halides is meager, limited to pseudo one-dimensional chalcogen-rich compounds such as $TaTe_4I$,[1] $(TaSe_4)_nI$ ($n = 2, 3$),[2,3] and $Ta_4Se_{16}Br_n$ ($n = 1, 2$)[3,4] and to the layered halide-rich compounds Ta_3SBr_7[5] and Ta_3QI_7 (Q = Se, Te),[6] recently discovered in our laboratory. A few others have been mentioned in the literature, with only cursory structural characterization. TaS_2Cl_2, $TaSCl_2$, $TaSCl_3$, $TaSBr_3$, and $TaSeBr_3$[7] have been assigned their various structural features on the basis of chemical analysis and metal-chalcogen stretching frequencies only. No tantalum sulfide iodide, to the best of our knowledge, has ever been reported. Certainly, the tally of ternary tantalum chalcogenide halide compounds lags well behind that of its lighter relative niobium, which has yielded a rich ternary chemistry. $NbTe_4I$,[8] $NbSeX_3$,[9,10] Nb_3QX_7,[11−16] NbSeI,[17,18] and Nb_6SI_9 [19] display remarkable structural diversity, adopting structures with isolated niobium atoms, Nb−Nb dimers, Nb_3 triangular clusters, Nb_4 tetrahedral clusters, and Nb_6 octahedral clusters, respectively. Additionally, centered Nb_6 trigonal prismatic clusters in the case of the alkali-metal salts $A_3Nb_6SBr_{17}$,[20,21] and tetranuclear butterfly clusters in $CsNb_4Cl_{11}$,[22] have been characterized. Generally, the metal atoms in these compounds can be assigned a single oxidation state (though occasionally a

---

* Author to whom correspondence should be addressed. E-mail: gmiller@iastate.edu.

[†] Current address: Department of Chemistry and Biochemistry, University of South Carolina, Columbia, SC 29210.

(1) Tremel, W. *Chem. Ber.* **1992**, *125*, 2165.
(2) Gressier, P.; Geumas, L.; Meerschaut, A. *Acta Crystallogr.* **1982**, *B38*, 2877.
(3) Gressier, P.; Meerschaut, A.; Guemas, L.; Rouxel, J.; Monceau, P. *J. Solid State Chem.* **1984**, *51*, 141.
(4) Grenouilleau, P.; Meerschaut, A.; Guemas, L.; Rouxel, J. *J. Solid State Chem.* **1987**, *66*, 293.
(5) Smith, M. D.; Miller, G. J. *J. Solid State Chem.* **1998**, *140*, 226.
(6) Smith, M. D.; Miller, G. J. *J. Am. Chem. Soc.* **1996**, *118*, 12238.
(7) Fenner, J.; Rabinau, A.; Trageser, G. *Adv. Inorg. Chem. Radiochem.* **1980**, *23*, 364.
(8) Deng, S.-Q.; Zhuang, H.-H.; Lu, C.-Z.; Huang, J.-S.; Huang, J.-L. *Acta Crystallogr.* **1993**, *C49*, 1135.
(9) Franzen, H. F.; Hönle, W.; von Schnering, H. G. *Z. Anorg. Allg. Chem.* **1983**, *497*, 13.
(10) Schmidt, P. J.; Thiele, G. *Z. Anorg. Allg. Chem.* **1999**, *625*, 1055.
(11) Miller, G. J. *J. Alloys Compd.* **1995**, *229*, 93.
(12) Furuseth, S.; Hönle, W.; Miller, G. J.; von Schnering, H. G. *9th International Conference on Solid Compounds of Transition Elements, Abstracts*; Royal Society of Chemistry: London, 1988.
(13) Miller, G. J. *J. Alloys Compd.* **1995**, *217*, 5.
(14) Khvorykh, G. V.; Shevelkov, A. V.; Dolgikh, V. A.; Popovkin, B. A. *J. Solid State Chem.* **1995**, *120*, 311.
(15) Schmidt, P. J.; Thiele, G.; Whangbo, M.-H. *Eur. J. Inorg. Chem.* **1999**, 785.
(16) Schmidt, P. J.; Thiele, G. *Acta Crystallogr. Sect. C* **1997**, *C53*, 1743.
(17) Fedorov, V. E.; Evstaf'ev, V. K.; Kirik, S. D.; Mishchenko, A. V. *Zh. Neorg. Khim.* **1981**, *26*, 2701.
(18) Ben-Yaich, H.; Jegaden, J. C.; Potel, M.; Sergent, M.; Rostogi, A. K.; Tournier, R. *J. Less-Common Met.* **1984**, *102*, 9.
(19) Meyer, J. H.; Corbett, J. D. *Inorg. Chem.* **1991**, *30*, 963.
(20) Womelsdorf, H.; Meyer, H. J. *Angew. Chem.* **1994**, *106*, 2022; *Angew. Chem., Int. Ed. Engl.* **1994**, *33* (19), 1943.
(21) Womelsdorf, H.; Meyer, H.-J. *Z. Anorg. Allg. Chem.* **1996**, *622*, 2083.
(22) Broll, A.; Simon, A.; von Schnering H.-G.; Schäfer, H. *Z. Anorg. Allg. Chem.* **1969**, *367*, 1.

10.1021/ic034075q CCC: $25.00

nonintegral one). Compounds made at higher temperatures seldom exhibit mixed-valent behavior, where the same metal exists in two different formal oxidation states in the same compound. A few examples from niobium chemistry are known, however. The binary halide Nb_3Cl_8 actually forms in the composition range $Nb_{3-x}Cl_8$ ($x \leq 0.44$)[23] and has been described as a mixed $(Nb^{4+})_2Cl_8/(Nb^{2.67+})_3Cl_8$ system.[12] $Nb_3Se_5Cl_7$ has been formulated $(Nb^{5+})(Nb^{4+})_2(Se_2^{2-})_2(Se^{2-})(Cl^-)_7$.[24] Another example is the peculiar compound $Nb_7S_2I_{19}$, where trigonal bipyramidal $(Nb^{5+})I_5$ molecules are encapsulated inside a layered $(Nb^{3+})_3SI_7$ framework.[25] In this compound, however, the NbI_5 units can almost be considered a kind of molecule of crystallization since they are encapsulated in large channels and are not directly joined to the extended Nb_3SI_7 framework. Such compounds, besides providing structural novelty, are also interesting examples of the delicate balance possible between competing redox forces within a structure.[26]

During the course of our studies of the ternary chalcogenide halide chemistry of tantalum, we have focused on halide-rich compositions, usually near Ta_3QX_7. As part of an attempt to synthesize Ta_3SI_7, we have discovered the novel mixed-valent compound Ta_4SI_{11}, containing both trinuclear Ta_3^{3+} clusters and isolated Ta^{4+} ions amid undulating, disordered sulfur and iodine layers. Herein, we report the synthesis as well as structural and theoretical characterization of this new structure type.

Experimental Section

Synthesis. Ta_4SI_{11} was first observed as an abundant (ca. 50%) side product from reactions of the elements in the molar ratio 3:1:7 Ta:S:I at 450 °C in sealed, evacuated borosilicate glass tubes, designed to grow Ta_3SI_7 phases. Because of the inability to identify the compound from its Guinier powder diffraction pattern, a single crystal was selected and its structure solved (see below), yielding the composition "Ta_4SI_{11}". Tubes were then loaded at this stoichiometry and heated at various temperatures to determine optimum synthetic conditions. Ta_4SI_{11} is best made by stoichiometric reaction of the elements at 430 °C, for a duration of 2 weeks. Growth of the compound is sensitive to temperature gradients in the tube: highest (nearly quantitative) yields were obtained when the tube furnace was packed tightly with asbestos, to smooth out uneven temperature regions as much as possible. Heating a Ta_4SI_{11} mixture with an imposed temperature gradient leads to a mixture of phases, including hexagonal and orthorhombic Ta_3SI_7, and Ta_6I_{14} in addition to Ta_4SI_{11}. The reagents used were tantalum "turnings" (Aesar, 99.99%, cleaned with an $HF/HNO_3/H_2SO_4$ solution to remove surface impurities, then rinsed with ethanol, and dried in vacuo at 500 °C), sulfur powder (Alfa, 99.9%, sublimed twice before use), and iodine (Alfa, 99.9%, resublimed). All purified reagents and products were handled in an Ar-filled glovebox.

Ta_4SI_{11} crystallizes as long silver bars, which often aggregate in dense thickets (Figure 1). The brittle crystals splinter easily along the long axis. Ta_4SI_{11} is sensitive to oxygen and moisture, decomposing to an uncharacterized white powder after several days. In inert atmospheres, the compound appears to be indefinitely stable toward decomposition up to temperatures of ≈525 °C, above which only Ta_6I_{14}, TaI_5, and TaS_2 are observed by X-ray powder diffraction.

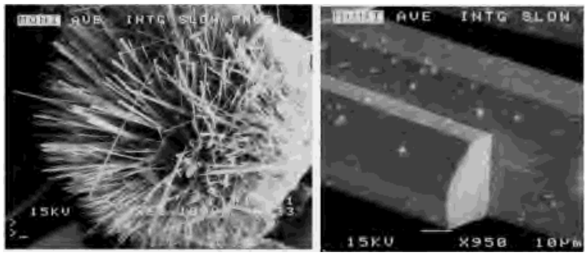

Figure 1. SEM images of (left) a typical spiny ball formation of Ta_4SI_{11}; (right) higher magnification of the end of a crystal.

Scanning Electron Microscopy. Verification of the presence of tantalum, sulfur, and iodine in multiple single-crystal samples of Ta_4SI_{11} was carried out using a JEOL 6100 scanning electron microscope operating at 15 kV.

X-ray Photoelectron Spectroscopy. XPS spectra were measured using a PHI 5500 multitechnique surface analysis equipment instrument, using Mg Kα radiation (29.35 eV). Samples were prepared by finely powdering several larger single crystals of Ta_4SI_{11} in the glovebox immediately before use. The samples were pressed onto indium foil in the glovebox and transferred to the XPS instrument via an inert atmosphere carrier. Binding energies were corrected for charging using the C 1s peak of adventitious carbon (284.8 eV) as an internal reference.[27] However, no significant charging effects were observed, as C 1s always appeared at 284.8 eV. Additionally, large intact single crystals were mounted and etched by sputtered Ar ions to remove any surface impurities introduced during handling, to probe the presumably pristine interior of the sample.

Magnetic Susceptibility. Temperature-dependent magnetic susceptibility measurements were performed with a Quantum Design SQUID magnetometer. Aggregations of Ta_4SI_{11} bars were loaded and sealed under an inert atmosphere in fused silica tubes. The samples were kept in place by means of two tightly fitting fused silica rods on either side of the sample. The samples were chosen so that only larger single-crystal aggregations were used, to avoid unwanted powder impurities and to minimize the surface area susceptible to oxidation. Measurements were taken from 4 to 300 K, at a field strength of 3 T. The results are shown in Figure 2. A room-temperature moment of 1.53 μ_B was measured, reproducible over three separate runs.

X-ray Crystallography. A small silver bar ($0.02 \times 0.03 \times 0.12$ mm^3) was sealed inside a glass capillary under argon and mounted on a Siemens P4 diffractometer. A primitive orthorhombic unit cell with dimensions $a = 16.135(3)$ Å, $b = 3.813(1)$ Å, and $c = 8.131(2)$ Å was indexed and refined on the basis of 45 reflections in the range $6° \leq 2\theta \leq 25°$. Axial photographs confirmed these lattice metrics. 2629 reflections were collected to $2\theta_{max} = 55°$, of which 685 were unique, 533 unique observed ($I > 2\sigma I$), and $R_{int} = 0.0498$. An empirical absorption correction was applied to the data, using the average of six complete "psi-scans" measured in well-separated regions of reciprocal space. The structure was solved using direct methods (SHELX-86) and refined with the SHELXL-93 crystal-

---

[23] Hulliger, F. In *Structural Chemistry of Layer-Type Phases*; Lévy, F., Ed.; Reidel: Dordrecht, 1976.

[24] Rijnsdorp, J.; Jellinek, F. *J. Solid State Chem.* **1979**, *28*, 149.

[25] Miller, G. J.; Lin, J. *Angew. Chem.* **1994**, *106*, 357; *Angew. Chem., Int. Ed. Engl.* **1994**, *33*, 334.

[26] Rouxel, J. *Comments Inorg. Chem.* **1993**, *14*, 207.

[27] Moulder, J. F.; Stickle, W. F.; Sobol, P. E.; Bomben, K. D. *Handbook of X-ray Photoelectron Spectroscopy*; Chastain, J., Ed.; Perkin-Elmer Corp.: Eden Prairie, MN, 1992.

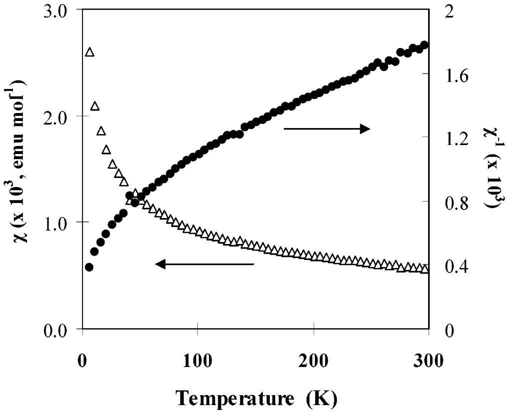

Figure 2. Temperature-dependent magnetic susceptibility for Ta_4SI_{11} (molar susceptibility χ, emu mol^{-1}, and inverse molar susceptibility χ^{-1}, mol emu^{-1}). A fit to Curie−Weiss behavior for temperatures exceeding 100 K gives $\mu_{eff} = 1.53\ \mu_B$.

Table 1. Summary of Crystallographic Data for Ta_4SI_{11}

fw	2151.76
space group	*Pmmn* (No. 59)
lattice params	
a (Å)	16.135(3)
b (Å)	3.813(1)
c (Å)	8.131(2)
vol (Å^3)	500.2(2)
Z	1
d_{calc} (g cm^{-3})	7.143
radiation	Mo Kα, $\lambda = 0.71071$ Å
linear abs coeff	38.854 mm^{-1}
temp	23 °C
residuals[a]	
R1 (observed/all data)	0.0322/0.0503
wR2 (observed/all data)	0.0695/0.0762

[a] $R1 = \sum||F_o| - |F_c||/\sum|F_o|$; $wR2 = [\sum w(F_o^2 - F_c^2)^2/\sum w(F_o^2)^2]^{1/2}$; $w = 1/\sigma^2(F_o)$.

Table 2. Important Internuclear Distances (Å) in Ta_4SI_{11}

atom−atom	distance (Å)
Ta1−Ta1	2.998(2)
Ta1−Ta2	3.157(1)
Ta1−I1	2.769(1) ×2
Ta1−I2	2.583(2); 3.127(2)
Ta1−I4	2.892(2)
Ta1−S	2.523(2)
Ta2−I1	2.744(1) ×2
Ta2−I3	2.780(1) ×2; 3.112(2)
Ta2−I4	2.286(1)
Ta2−S	2.324(5)

lographic package.[28,29] Further data collection details and important internuclear distances are given in Tables 1 and 2, respectively.

Results and Discussion

Figure 3 shows a 80% probability displacement ellipsoid plot of the local Ta environments in Ta_4SI_{11}, representing the $(Ta_3)^{9+}/Ta^{4+}$ disorder model discussed below. Figure 4a shows Ta_4SI_{11} viewed parallel to the short *b* axis. The compound can be viewed as a close-packed structure similar to the M_3QX_7 compounds, but with a different metal atom distribution. In Ta_4SI_{11}, approximately close-packed layers of composition "SI_{11}" stack parallel to the $(\bar{3}02)$ family of lattice planes in cubic close-packed ((...*ABC*...) or (...*c*...)) fashion, at an angle of 37.25° from the *a* axis.

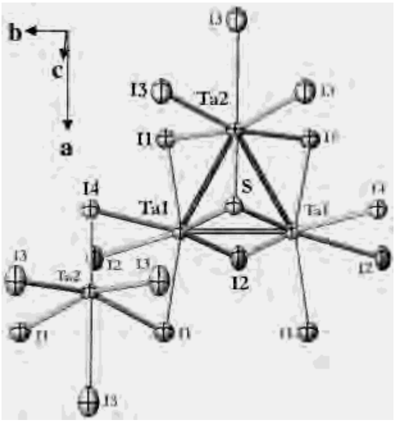

Figure 3. Displacement ellipsoid view (80% probability) and atom labeling scheme showing the Ta_3 clusters and isolated Ta centers hypothesized to be disordered throughout the structure of Ta_4SI_{11}. Independent atomic positions are labeled in bold; symmetry-equivalent positions are smaller and gray.

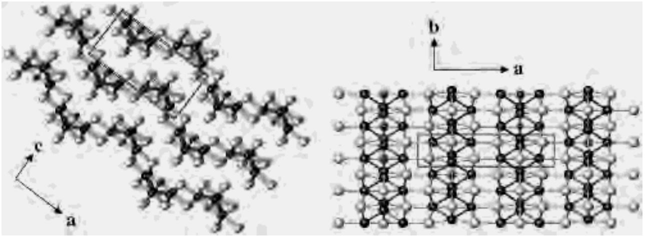

Figure 4. (a) [010] projection of Ta_4SI_{11}. Larger black circles are Ta atoms; smaller black circles are S atoms; large white circles are I atoms. (b) [001] projection of Ta_4SI_{11}. Both figures illustrate all fully and partially occupied positions. In the [001] projection, it is clear that two Ta sites cannot be simultaneously occupied.

However, instead of a pattern of interstitial site occupation by the metal atoms that generates flat parallel slabs as in the layered M_3QX_7 compounds, in Ta_4SI_{11} the occupation of these sites defines an undulating sheet structure with a period of 16.135 Å. Ta_4SI_{11} can still be viewed as a "layered" structure since the undulating Ta_4SI_{11} layers are separated by a van der Waals gap.

The nature of the distibution of tantalum atoms within the layers is not straightforward. The structure solution gives rise to two crystallographically distinct tantalum positions. Full occupation of these sites would lead to butterfly Ta_4 clusters that bend at the turns of the undulating anion layers. However, the site occupation factors of both metal sites each refine to near 50%. An additional complication is the atomic position at the cradle or elbow of the apparent bent cluster, seemingly bridging all four metals. This site refines as a 50:50 sulfur−iodine split position (S/I4). Figure 4b shows a [001] view of what the crystallographic experiment sees, which is an average over the entire crystal. The question now becomes how the metal atoms are distributed throughout the structure and how the metal atom distribution correlates with the split S/I4 position. We can attribute the various site occupancies to structurally ordered ribbons of Ta clusters, shown in Figure 5, with the distribution of ribbons along [100] as well as along different layers in the layer stacking

---

(28) Sheldrick, G. M. *SHELX-86*; University of Göttingen: Göttingen, Germany, 1986.

(29) Sheldrick, G. M. *SHELXL93 Program for the Refinement of Crystal Structures*; University of Göttingen: Göttingen, Germany, 1993.

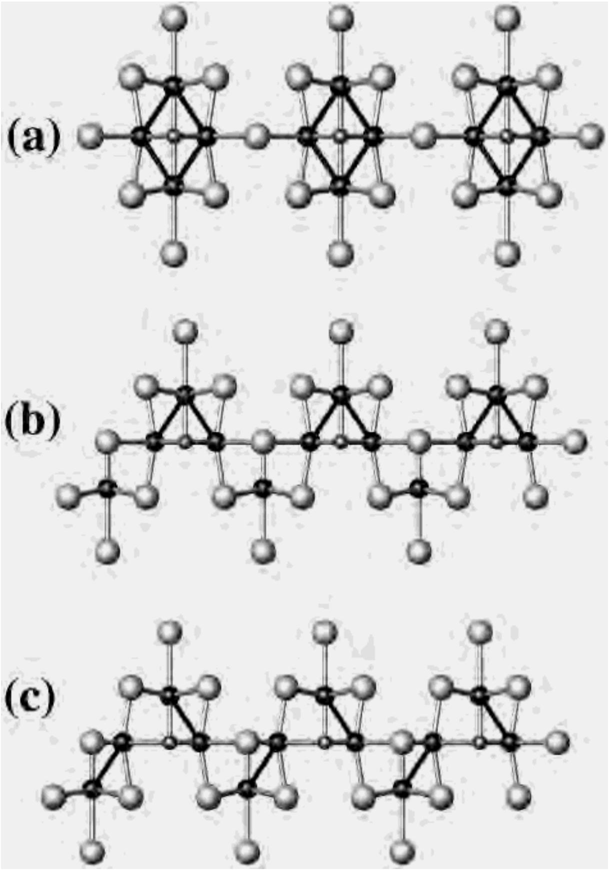

Figure 5. Three possible distributions of Ta atoms that may exist in Ta_4SI_{11}. (a) "Butterfly" clusters; (b) triangles alternating with isolated Ta atoms; (c) herringbone pattern of Ta_2 dimers.

([001]) direction being completely disordered. Within a ribbon along [010], there are three possibilities for the distribution of Ta atoms (see Figure 5): (1) Ta_4 "butterfly" clusters linked by bridging S/I4 ions; (2) alternating Ta_3 triangular clusters and isolated Ta atoms; and (3) a "herringbone" pattern of Ta_2 dimers. The distribution of S and I4 atoms should be closely correlated with the patterns of Ta clusters in possibilities (1) and (2), but less so for possibility (3). The solution to this problem cannot be conclusively determined based on the X-ray diffraction experiment, which measures average electron density over the entire crystal and cannot elucidate the precise local situation: independent characterization methods are required.

X-ray Photoelectron Spectroscopy. To help clarify more details about the structure, X-ray photoelectron spectroscopy spectra were measured. The XPS spectrum of any tantalum atom produces a doublet signal, corresponding to the $4f_{7/2}$ (lower binding energy) and $4f_{5/2}$ (higher binding energy). These peaks are always separated by 1.91 eV. This constant separation facilitates deconvolution of overlapping peaks due to inequivalent atoms. The binding energies reported below are for the Ta $4f_{7/2}$ peaks. The Ta_4SI_{11} spectrum showed two peaks at 23.8 and 26.3 eV with visibly different integrated intensities (the intensity of the 23.8-eV peak is noticeably greater than that of the 26.3-eV peak), which suggest two different oxidation states for Ta in different concentrations. The Ta $4f_{7/2}$ binding energy of 23.8 eV indicates a reduced metal center and suggests the presence of triangular clusters having an average oxidation state of +3. The binding energies of Ta in *hc*-Ta_3SeI_7 and *hc*-Ta_3TeI_7, which contain Ta_3 clusters, are 23.4 eV.[6] For comparison, literature XPS values[27] for tantalum in other compounds are listed in Table 3. It is also possible to assign the peak at 26.3 eV to oxygen contamination of the sample, and not to a mixed-valence effect within the compound. However, oxygen contamination of the crystalline samples used would be limited to surface oxidation since all products were handled under an inert atmosphere. To explore this possibility, samples of single crystals were etched in the XPS instrument by sputtering with Ar ions. Etching removes contaminated surface layers and exposes the nonoxidized, presumably pristine interior of the sample. After etching, the peak at 26.3 eV persisted, which suggests this peak is characteristic of the sample, and not due to surface oxidation. Additionally, the Ta $4f_{7/2}$ peak of Ta_2O_5 appears at slightly higher binding energy (26.7 eV, Table 3).

Table 3. Tantalum $4f_{7/2}$ Binding Energies (eV) Measured by X-ray Photoelectron Spectroscopy

compound	binding energy (eV)
Ta metal	21.6−21.9
$(NEt_4)_2[Ta_6Cl_{12}]Cl_6$	23.8
$[Ta_6Cl_{12}]Cl_2(H_2O)_4\cdot 4H_2O$	25.8
K_3TaO_4	25.9
TaS_2	26.7
Ta_2O_5	26.7
$TaBr_5$	26.9
K_2TaF_7	29.4
hc-Ta_3SeI_7[6]	23.4
hc-Ta_3TeI_7[6]	23.4

The two binding energies suggest a mixture of Ta_3 trinuclear clusters and tantalum atoms in a higher oxidation state. It is not likely that the two peaks result from chemical inequivalencies within the trinuclear cluster itself (local symmetry C_s), as the 2.8-eV difference between the two is much too large to support this contention. The distortion of the Ta_3 clusters away from perfect equilateral geometry is moderate, with Ta−Ta distances of 3.157(2) and 2.999(2) Å and angles of 56.70(1)° and 61.65(1)°. A formulation of Ta_4SI_{11} consistent with the crystallographic, magnetic, and X-ray photoelectron spectroscopic data is "$(Ta^{3+})_3(Ta^{4+})(S^{2-})(I^-)_{11}$"; a 1:1 mixture of Ta_3 clusters and isolated Ta atoms in the +4 oxidation state. These two metal species must be randomly distributed throughout the three-dimensional structure to give the apparent averaged structure solved from the X-ray diffraction data. While it is possible (but, as yet, unverifiable) that some kind of ordering of the trinuclear clusters and isolated atoms exists within each undulating layer, certainly no ordering or registry can exist between the Ta_4SI_{11} layers; otherwise, different symmetry, unit cell, or superstructure reflections would be found. This formulation is also bolstered by the magnetic data, where the derived magnetic moment of 1.53 μ_B indicates one unpaired electron per formula unit, close to the spin-only value for isolated d^1 Ta^{4+} centers.

The assignment of the split sulfur−iodine position remains, but we hypothesize an arrangement commensurate with the pattern of trinuclear clusters given our experience with

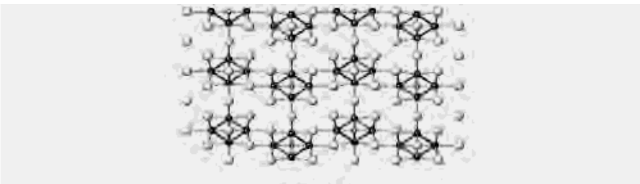

(a) Model 1

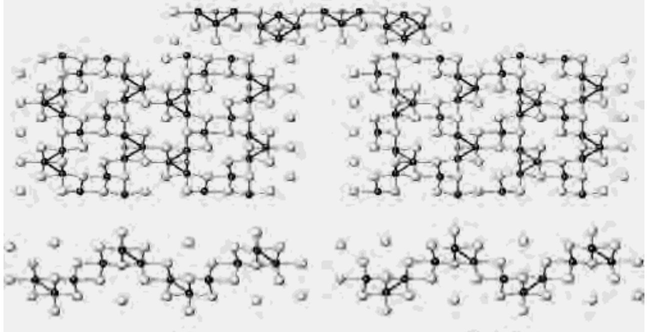

(b) Model 2

(c) Model 3

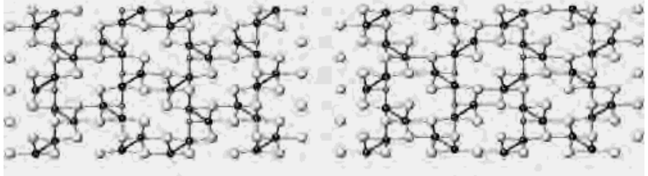

(d) Model 4

(e) Model 5

Figure 6. Five different structural models of Ta atom distribution used for extended Hückel calculations of total energies.

various M_3YX_7 compounds. Therefore, at each trinuclear cluster, sulfur is the capping atom. Conversely, then, when the single tantalum atom occurs, it is surrounded by an octahedral coordination environment of entirely iodine. This assignment accounts for the amount of each species present in this structure, as well as being the most reasonable placement of the sulfur atoms in light of the behavior of the chalcogen in the similar compounds Ta_3QX_7,[6] that is, always capping a trinuclear cluster. While most Ta−I and Ta−S bond distances are typical,[5,6] there is, however, an extremely short Ta2−I4 bond length of 2.286(1) Å, around the Ta^{4+} ions. However, with the disorder and fractional occupancy present throughout the structure, such a distance could be a false artifact forced upon the structure as a consequence of averaging. No unusual motion is manifest in the anisotropic displacement parameters for S or I4 (see Supporting Information). The only noticeably large U_{ij} value is U_{33} for I2, apparently elongated into the van der Waals gap.

Extended Hückel Calculations. Extended Hückel calculations were carried out on five structural models (illustrated in Figure 6a−e) of the Ta_4SI_{11} structure based upon the three models enumerated above, using atomic orbital parameters given in Table 4. The purpose of these calculations was to determine the total energies of various possible metal atom distributions. The unit cells for all five models utilized doubled *b* axis lengths to account for the Ta positions along the ribbons but kept the observed values of *a* and *c* axes lengths. The five models are (view normal to the layers in all cases with additional [010] views for 6b and 6c):

Model 1: "Butterfly" Ta_4 clusters, distributed over the three-dimensional structure as shown in Figure 6a. Along the [010] direction of each undulating Ta_4SI_{11} layer, a Ta_4 cluster is fully occupied, with the adjacent Ta_4 set unoccupied. For this model, the sulfur was positioned in the crook of the cluster, coordinated to all four Ta atoms.

Table 4. Atomic Orbital Parameters Used in Extended Hückel Calculations on Different Models of Ta_4SI_{11}

atom	orbital	H_{ii} (eV)	ζ_1	c_1	ζ_2	c_2
Ta	6s	−8.96	2.28			
	6p	−4.99	2.24			
	5d	−9.83	4.76	0.6104	1.94	0.6104
S	3s	−20.00	2.12			
	3p	−13.30	1.83			
I	5s	−18.00	2.66			
	5p	−12.72	2.32			

Models 2 and 3: A 50:50 mixture of Ta_3 clusters and isolated Ta atoms. There are two possible unique distributions in this case: (Figure 6b) such that the Ta_3 clusters are all parallel throughout the structure when viewed along [010], or (Figure 6c), the Ta_3 clusters alternate orientation, following the undulating layers.

Models 4 and 5: A "herringbone" pattern of Ta_2 dimers along [010], with each dimer bridged by a sulfur atom and an iodine atom (Figure 6d,e).

The calculations showed a significant energetic separation among the three broad cases: the total energies of the two $Ta_3 + Ta$ cases (Figure 6b,c) were found to be quite similar, differing by only 0.07 eV (per formula unit) from one another. However, both of these cases were clearly stabilized relative to the butterfly clusters by 0.27 eV per formula unit and to the dimers by 1.57 eV.

Ta_4SI_{11} bears a structural resemblance to the novel niobium sulfide iodide *o*-Nb_3SI_7.[11] Both structures contain undulating mixed sulfur−iodine layers, with the metal atoms defining a similar undulating layer structure. Within both undulating layer structures, triangular clusters are capped by a sulfur atom, generating local M_3X_{13}-type clusters. In *o*-Nb_3SI_7, the Nb_3 cluster coordination environment involves an additional sulfur atom; this second coordinating S provides a bridge to another Nb_3 cluster. Coordination of the Nb_3 units is then "$Nb_3S_2I_{11}$". In Ta_4SI_{11}, the sulfur atom is not shared between separate clusters, and the Ta_3 coordination is "Ta_3SI_{12}". Because of these structural similarities, and considering the crystallographic difficulties encountered in the solutions of both structures, one might raise the possibility of whether Ta_4SI_{11} might actually be "*o*-Ta_3SI_7", isostructural with the Nb case, but with a disorder mechanism falsely but reproducibly generating two different solutions. In fact, we have also synthesized a compound whose powder pattern is virtually the same as that of *o*-Nb_3SI_7, though diffraction quality single crystals have not been grown.[30] Examination of Guinier X-ray powder diffraction patterns of pure samples of Ta_4SI_{11} and "*o*-Ta_3SI_7" as well as the powder pattern from the published *o*-Nb_3SI_7 structure was definitive in establishing the uniqueness of the two structure types. It is clear that the patterns are significantly different, reflecting the different structures that emerge from the single-crystal structure determinations.

---

[30] Smith, M. D.; Miller, G. J. Unpublished results.

The available data support the contention of a mixed-valent, disordered sulfide iodide. The problem of the short Ta2−I4 distance remains and is a disturbing one. Other attempts at characterizing the sample have been attempted: Various mass spectrometry techniques (electron impact ionization and chemical ionization in positive and negative ion modes) have been employed, but the compound is not sufficiently volatile to produce any vapor-phase fragments that could illuminate structural details. The compound is not soluble without decomposition, and therefore other ionization techniques (electrospray, etc.) cannot be used. The potential of an undetected superstructure exists. In particular, the split position might be “frozen” or resolved into one position, giving rise to an ordered structure. Examination of several crystals at low temperature, using both a rotating anode X-ray source and CCD area detector data, did not reveal either a different unit cell or superstructure reflections that would indicate a structural change from that reported herein.

Supporting Information Available: X-ray crystallographic data in CIF format. This material is available free of charge via the Internet at http://pubs.acs.org.

IC034075Q